Korean J. Chem. Eng., **31**(7), 1120-1135 (2014)
DOI: 10.1007/s11814-014-0038-y

pISSN: 0256-1115
eISSN: 1975-7220

Performance enhancement and energy reduction using hybrid cryogenic distillation networks for purification of natural gas with high CO_2 content

Khuram Maqsood, Jayita Pal, Dhanaraj Turunawarasu, Anindya Jyoti Pal, and Saibal Ganguly†

Chemical Engineering Department, Universiti Teknologi PETRONAS, Bandar Seri Iskandar, 31750, Perak, Malaysia
(*Received 12 March 2013 • accepted 1 February 2014*)

Abstract−A novel concept of hybrid cryogenic distillation network has been explored which maximizes the benefits of both desublimation or solid-vapor based separation as well as distillation or vapor-liquid equilibrium based separation during the separation of carbon dioxide from methane or natural gas. Process network synthesis has been performed for four case studies with high carbon dioxide (72 mole%) and medium carbon dioxide (50 mole%) natural gas feed streams. The benefits of optimal locations for cryogenic packed beds were investigated. A conventional cryogenic network consisting of multiple distillation columns with butane as additive for extractive distillation was also studied and presented in this paper. Process modeling of cryogenic distillation network with MESH equations was attempted using an integrated dual loop (C+3) convergence and the results were compared with Aspen Plus simulator for benchmarking. The prediction of solidification region was employed using experimental data from literature to avoid solidification regions in the column. The proposed hybrid cryogenic distillation network showed promising potential for energy and size reduction.

Keywords: Hybrid Cryogenic Distillation Network, Modeling, Natural Gas Purification, CO_2 Capture

INTRODUCTION

Natural gas provides one of the most useful and widely utilized energy sources of the world; however, it contains impurities like water, sand, carbon dioxide, hydrogen sulfide, wax, higher hydrocarbons, natural gas liquids and mercury [1]. While substantial literature exists for removal of hydrocarbons and sulfur containing gases at atmospheric pressures, considerable amount of research work needs to be focused on the removal of carbon dioxide particularly at high pipeline pressures up to 60 to 80 bars. With increasing energy demand, development of reserves with high CO_2 content up to 80% has become imperative requiring new research efforts. In Malaysia, an enormous amount of natural gas is undeveloped because of the high concentration of CO_2 often exceeding 70 mole% [2].

Researchers have reported work on chemical reagents and additive-based absorption, adsorption and membrane filtration techniques for removal of carbon dioxide. Utilization of chemical-based technologies become difficult and expensive in high sea offshore platforms with increasing amounts of carbondioxide in the natural gas. The present work highlights the use of cryogenic distillation and hybrid cryogenic separation networks for separation of CO_2 from natural gas.

In the present study, Malaysian natural gas with high CO_2 content has been cited to benchmark the potential of cryogenic separation networks. Solidification of CO_2 in the pipelines and columns in the gas processing plants may lead to blockage and may obstruct the transportation system. It can also reduce the selling price of gas by reducing the heating value. Therefore, the purification process has become an important step in natural gas processing [3].

Cryogenic separation has the additional advantage that it enables direct production of liquid CO_2 and transportation through pipelines, and is considered as one of the most promising methods of separating CO_2 from CH_4. The high relative volatility of methane with respect to carbon dioxide makes such processes theoretically attractive. The thermodynamic phase behavior of methane and carbon dioxide mixture has been reported and analyzed in literature [4-7]. However, the disadvantage that solid CO_2 exists in equilibrium with vapor liquid mixture of CH_4-CO_2 at particular conditions of pressure, temperature and composition presents the research challenges in this method.

Although cryogenic separation has been known in principle for quite some time in literature, proper and detailed quantitative research on the optimized complex cryogenic networks have only started recently in literature after the advancements of high-speed microprocessors and simulation techniques. The simulation of cryogenic separation networks involves sophisticated numerical computations on large interconnected process networks. The cryogenic processes for the separation of CO_2 from natural gas can be classified as conventional and non-conventional.

Conventional cryogenic distillation methods originated in literature with the Ryan/Holmes [8] process, which is an extractive distillation process used to overcome the problem of CO_2 solidification in the distillation column. The addition of heavier hydrocarbon (typically C_2-C_5) to the condenser of the distillation column was employed by Holmes et al. [9] to avoid CO_2 solidification. Recently, a three distillation column network using C_5 as an additive was simulated by Berstad et al. [10] using Aspen HYSYS for the separation of carbon dioxide from natural gas. Helium can also be used as an additive to facilitate the separation of CO_2 from methane and avoiding the carbon dioxide solidification [11]; however, the separation of

†To whom correspondence should be addressed.
E-mail: gangulysaibal2011@gmail.com

He from CH_4 at higher pressure is quite difficult. A dual pressure distillation process to remove high concentration of carbon dioxide from methane was reported by Atkinson et al. [12] that consists of two columns with different operating pressures. The overhead product of the second column produces methane for pipeline specification, but the pressures of these columns must be carefully selected to avoid CO_2 solidification. Process information is hardly available for further development or commercialization of this process.

Nonconventional cryogenic separation methods, contrary to the conventional cryogenic distillation processes, encourage formation of solid carbon dioxide. CFZ (Controlled freeze zone) technology [13,14] developed by ExxonMobil for handling a wide range of CO_2 and H_2S concentration, deliberately encourages formation of solid CO_2. The CFZ tower consists of an upper rectification section and lower stripping section, and these two are separated by a CFZ section. The height of the tower makes it difficult to use for offshore applications and loss of hydrocarbons needs further research under higher pressures. Cryocell technology [15] was developed and tested in a demonstration plant in Australia. It consists of controlled freezing and subsequent remelting of CO_2. Detailed simulation and separation characteristics using a cryocell technology are scarce in literature. Tuinier et al. [16] reported novel dynamically operated packed bed on the basis of dew and sublimation temperatures and an effective separation of CO_2 was achieved without any plugging problem and pressure drop. Considerable research efforts are still required to develop optimized cryogenic dynamic bed separation for natural gas, particularly at higher pressures, which have still not been reported in literature. A two-stage compression, refrigeration and separation process has been developed for the liquefaction and separation of carbondioxide [17]. Compression and refrigeration leads to higher exergy loss and almost 90% CO_2 can be separated. Some recently reported [18-20] cryogenic CO_2 removal technologies, comprised of mechanical methods to separate the CO_2 rich phase from the natural gas. A process of C3sep (condensed contaminant centrifugal separation), in which CO_2 is condensed into droplets and then separated from the natural gas by using rotational separators [18]. A process of frosting and defrosting of CO_2 on mechanical fins of heat exchanger based on a 4-stage integrated cascade was proposed by Clodic et al. [19]. Another cryogenic system for CO_2 capture based on the condensation and desublimation by the use of stirling coolers has been studied and tested [20,21]. In the desublimation step, the frost layer on the heat exchanger surface significantly reduces the heat transfer and a long time is needed to reach the required cryogenic conditions. Fluor Enterprises Inc. also developed a CO_2 liquefaction process called CO_2LDSEP [22]. This technology includes a series of compression and expansion steps to liquefy the carbon dioxide and separate it from hydrogen.

Experimental studies using single cryogenic packed bed and multiple cryogenic beds for separation of water and carbon dioxide from natural gas at normal pressures have been recently reported by Nor Syahera et al. [23] and Abulhassan et al. [24,25]. The authors have shown substantial separations till the operational saturation of the cryogenic beds, after which the cryogenic beds are switched by the supervisory control system for regeneration and cooling. The authors

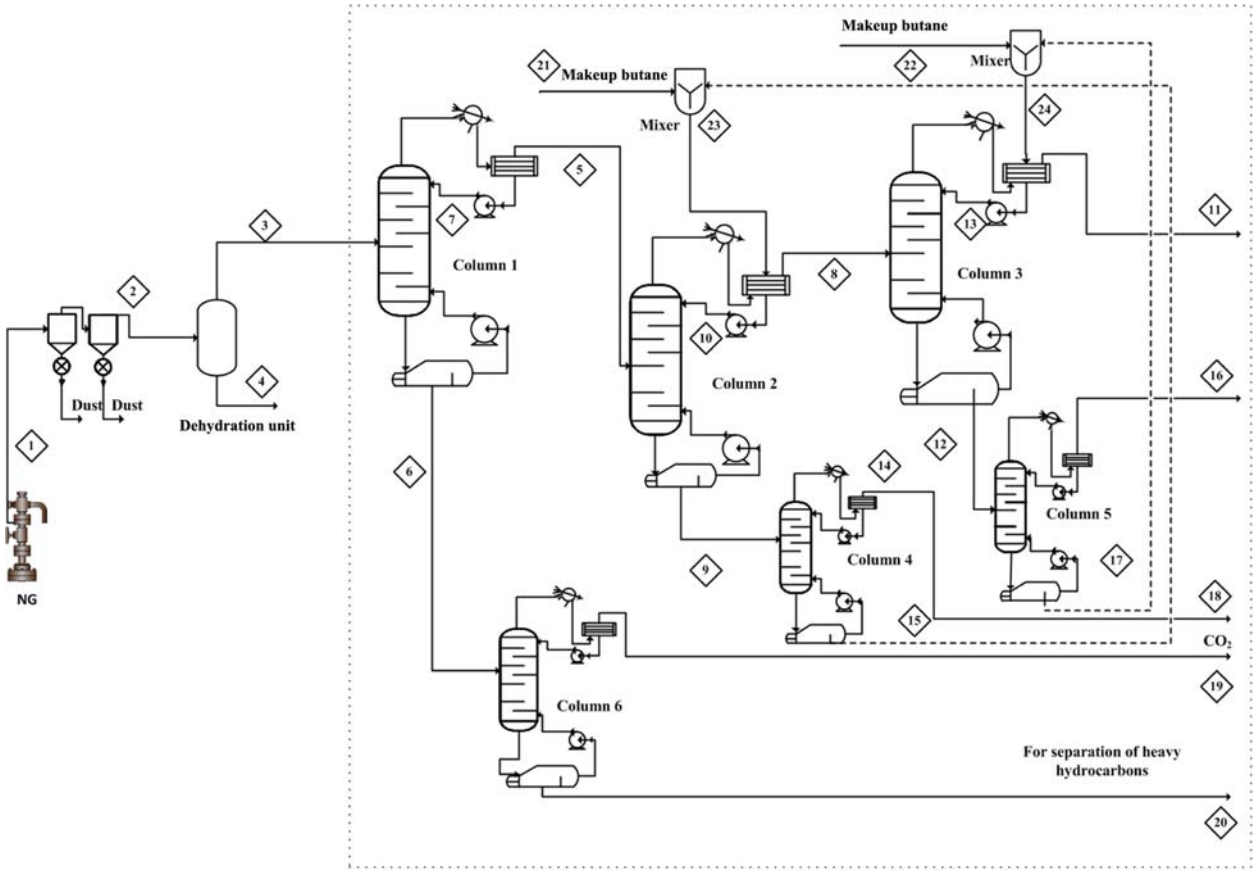

Fig. 1. Schematic of conventional cryogenic distillation process for natural gas purification (base case).

have also shown that the multiple cryogenic packed beds have potential for reducing energy requirements [23,24]. Note that the heavier hydrocarbons in natural gas passes into the liquid phase under cryogenic temperatures at high pressures. Therefore, optimized selection of bed pressure and temperature conditions based on feed gas composition becomes imperative while using this method.

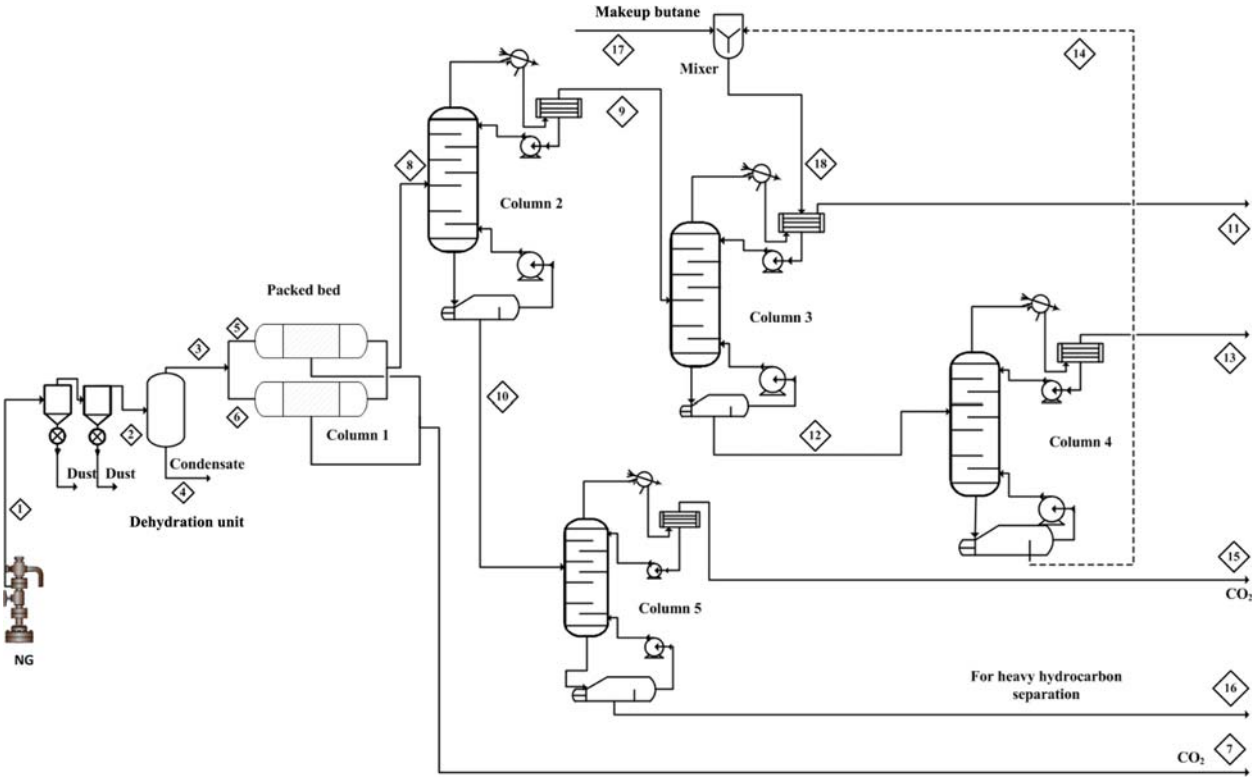

Fig. 2. Schematic of hybrid cryogenic distillation process for natural gas with 50 and 72 mole% CO_2 (case studies 2 and 3).

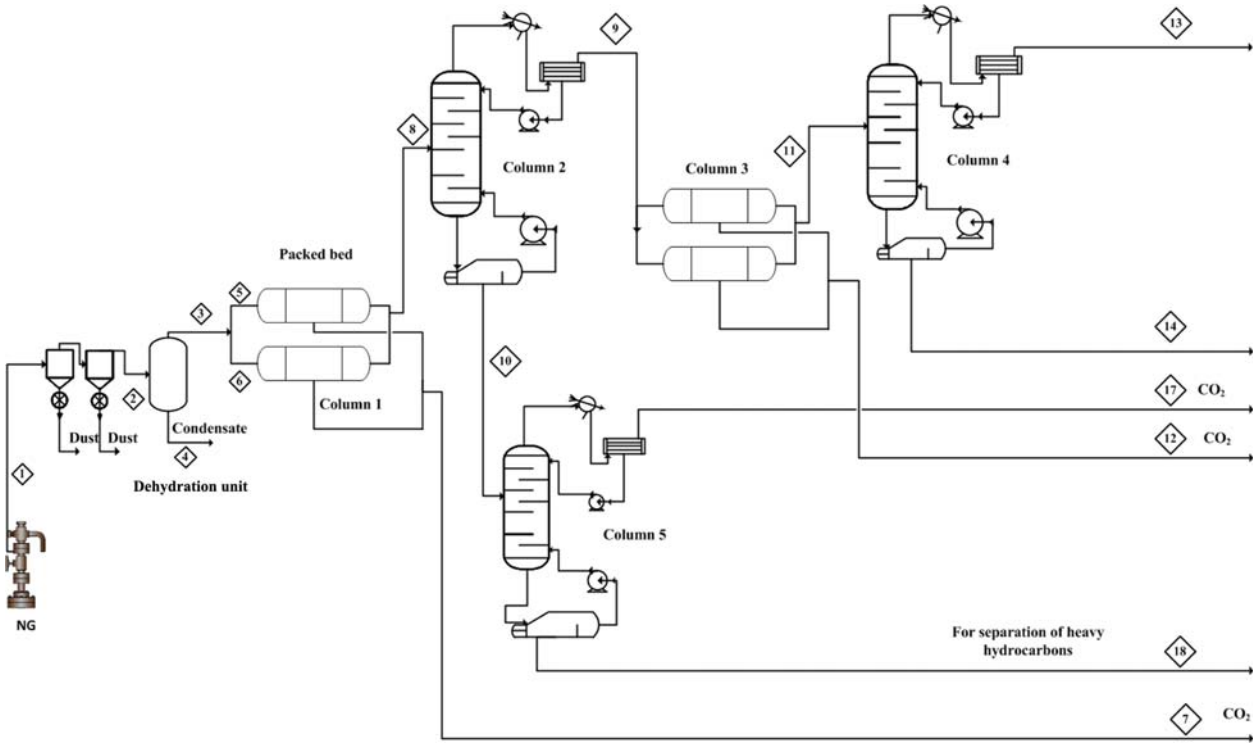

Fig. 3. Schematic of hybrid cryogenic distillation process for natural gas with 72 mole% CO_2 (case study 4).

A conventional cryogenic distillation network based process flowsheet was studied as the base case (Fig. 1) and propose a hybrid cryogenic network consisting of conventional cryogenic distillation network in conjunction with desublimation based multiple packed bed cryogenic separators. A schematic of the proposed networks is shown in Figs. 2 and 3. Three case studies have been performed to outline the benefits of using hybrid cryogenic networks to improve separation performance and reduce energy and size requirements. The effects of locating multiple cryogenic bed separators at different locations of the network have also been explored in the present work.

PROCESS SYNTHESIS FOR HYBRID CRYOGENIC SEPARATION NETWORKS

A hybrid system can be defined as a process system that involves different unit operations interlinked and optimized as one network to achieve a specified task. A hybrid cryogenic network for the purification of natural gas is presented in the current study that is a combination of a conventional cryogenic distillation network and the multiple cryogenic packed bed separators proposed by Abulhassan et al. [24,25]. Two different feeds with 50 mole% and 72 mole% carbon dioxide have been used for the present study and reported in Table 1. The hydrocarbon rich pure feed has not been considered in the present study and has been discussed elsewhere [26].

The concept of multiple bed cryogenic separators is best explained using the experimental data from Donnely and Katz [4], presented in Figs. 4 and 5. For a mixture of methane and carbon dioxide, a solidification region exists at pressure lower than 50-55 bars for different temperature ranges. With lowering of the pressure, the vapor-solid region increases as represented by Figs. 4 and 5. In Fig. 4, the solid region is represented by ABCD. The decrease in pressure also lowers the vapor-liquid region at lower concentration of carbon dioxide. It is evident from Figs. 4 and 5 that operation of distillation columns and the resultant separation becomes difficult at lower pressures without solidification of carbon dioxide. This phenomenon offers a research challenge to attain the required methane and carbon dioxide purity through separation network selection and operation at appropriate ranges of operating pressures and temperatures. The higher concentration of carbon dioxide present in the Malaysian natural gas and the final purity of methane required with acceptable energy usage make it difficult to use either of these processes individually. The proposed hybrid cryogenic network can deal with these problems more efficiently.

Table 1. Feed composition

Component	Feed composition	
	Case 1 (50% CO_2) [10]	Case 2 (72% CO_2) [2]
CH_4	0.397	0.20
C_2H_6	0.035	0.025
C_3H_8	0.024	0.015
n-C_4H_{10}	0.009	0.01
i-C_4H_{10}	0.009	0.01
n-C_5H_{12}	0.006	0.005
i-C_5H_{12}	0.006	0.005
C_6H_{14}	0.002	0.005
CO_2	0.506	0.72
N_2	0.005	0.005

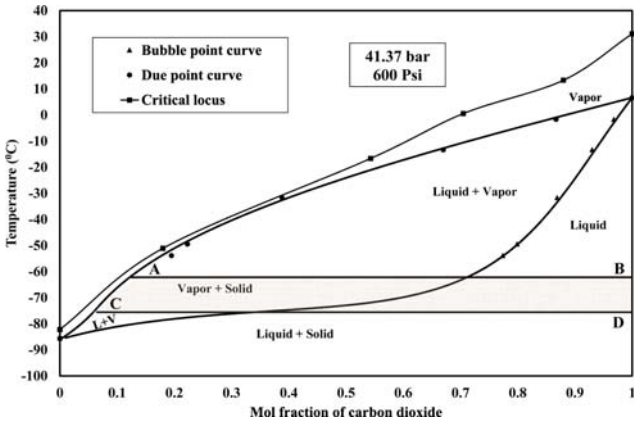

Fig. 4. Temperature-composition diagram of CH_4-CO_2 system at 41.37 bar [4].

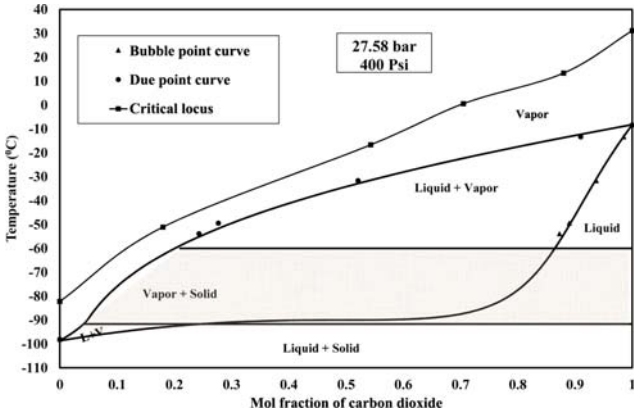

Fig. 5. Temperature-composition diagram of CH_4-CO_2 system at 27.58 bar [4].

Two hybrid cryogenic separation networks have been identified and presented in Figs. 2 and 3. In the first hybrid network (Case study 2 and 3), only a single cryogenic packed bed is employed at an appropriate location. In the second hybrid network (Case study 4), two cryogenic packed beds have been employed at appropriate locations.

MODELING AND SIMULATION OF HYBRID CRYOGENIC SEPARATION NETWORKS

The modeling of hybrid cryogenic networks essentially consists of the unconventional semibatch cryogenic packed beds operating under a cooling cycle, a capture cycle and a regeneration cycle along with the more conventional continuous distillation column networks operating in series. The models for the two types of operations have been summarized in the following sections.

1. Modeling of Conventional Distillation Columns

A generalized integrated dual loop convergence algorithm has been proposed to solve MESH equations for natural gas and carbon dioxide system. The model equations for an ordinary equilibrium stage of a simple distillation column, commonly known as mass balance, equilibrium, summation and enthalpy balance (MESH) equa-

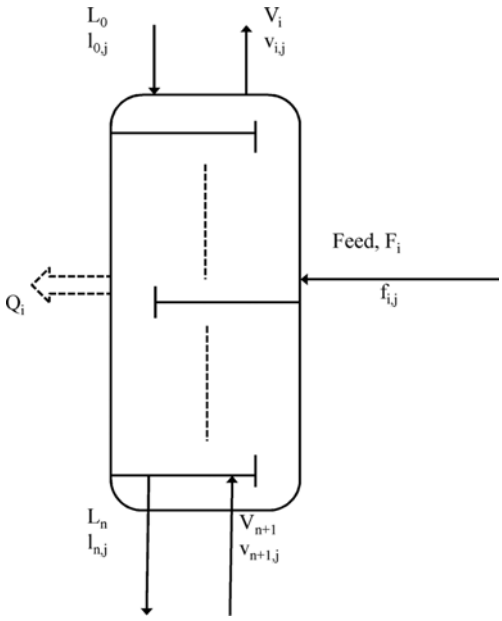

Fig. 6. Schematic diagram of stagewise distillation column variables.

tions, have been reported by several authors [27-30]. These fundamental equations are available in literature in terms of different nomenclatures and variable definitions to facilitate numerical stability and ease of convergence.

Fig. 6 shows a schematic representation of a general distillation stage along with its variables.

Total material balance for ith stage

$$(L_i - L_{i-1}) + (V_{i+1} - V_i) + F_i = 0 \tag{1}$$

Component material balance equation on ith stage for jth component

$$(l_{i-1,j} - l_{i,j}) + (v_{i+1,j} - v_{i,j}) + f_{i,j} = 0$$
$$i = 1,2,\ldots\ldots,N, \quad J = 1,2,\ldots\ldots,C \tag{2}$$

Equilibrium relation for jth component on ith stage

$$y_{i,j} = \eta_{i,j} K_{i,j} x_{i,j} \tag{3}$$

Energy balance equation for ith stage

$$\sum l_{i-1,j} h_{i-1,j} + \sum v_{i+1,j} H_{i+1,j} - \sum l_{i,j} h_{i,j} - \sum v_{i,j} H_{i,j} + \sum f_{i,j} h^F_{i,j} \pm Q_i = 0 \tag{4}$$

$$\text{Let } x_i = \begin{bmatrix} l_{i1} \\ l_{i2} \\ l_{i3} \\ \vdots \\ l_{iC} \\ v_{iC+1} \\ v_{iC+2} \\ \vdots \\ v_{i2C} \\ T_{i2C+1} \end{bmatrix} = \begin{bmatrix} x_{i1} \\ x_{i2} \\ x_{i3} \\ \vdots \\ x_{iC} \\ x_{iC+1} \\ x_{iC+2} \\ \vdots \\ x_{i2C} \\ x_{i2C+1} \end{bmatrix} \tag{5}$$

In Eq. (5), x_i represents the generalized Naphtali and Sandholm [30] structure of plate wise variable pairing with N x (2C+1) simultaneous convergence. The ease of convergence with (C+3) integrated dual loop convergence for complex distillation column flowsheets has been reported in literature [27].

From Eq. (3)

$$v_{ij} = S_{ij} l_{ij} \tag{6}$$

where S_{ij} is termed as the Stripping factor.

The functions for plate i [Eqs. (2), (3) and (4)] involve only the variables on plates i−1, i, and i+1. Thus the partial derivatives of the functions on this plate with respect to the variables on all plates other than these three are zero.

For component j, the matrix is represented by:

$$\begin{bmatrix} -1+S_{1,1} & S_{1,2} & 0 & 0 & 0 & 0 \\ 1 & -(1+S_{2,2}) & S_{2,3} & 0 & 0 & 0 \\ 0 & 1 & -(1+S_{3,3}) & S_{3,4} & 0 & 0 \\ \vdots & \vdots & \vdots & \vdots & \vdots & \vdots \\ 0 & 0 & 0 & 0 & 1 & -(1+S_{N-1,N-1}) \\ 0 & 0 & 0 & 0 & 0 & 1 \end{bmatrix}$$

$$\begin{bmatrix} 0 \\ 0 \\ 0 \\ \vdots \\ S_{N-1,N} \\ -(1+S_{N,N}) \end{bmatrix} \begin{bmatrix} l_1 \\ l_2 \\ l_3 \\ \vdots \\ l_{N-1} \\ l_N \end{bmatrix} = - \begin{bmatrix} f_1 \\ f_2 \\ f_3 \\ \vdots \\ f_{N-1} \\ f_N \end{bmatrix} \tag{7}$$

This formation is a tri-diagonal matrix form and is solved using the Thomas algorithm to generate the component liquid flow rates in the column. This constitutes the inner loop of the dual loop structure.

For the i^{th} stage of a multi-component distillation problem for a simple column, the (C+3) formulation uses $x_{i,j}$, L_i, V_i and T_i as independent variables to write the following equations.

Mass balance

$$(L_i - L_{i-1}) + (V_{i+1} - V_i) + F_i = \mathcal{D}_p \tag{8}$$

Energy balance

$$\sum l_{i-1,j} h_{i-1,j} + \sum v_{i+1,j} H_{i+1,j} - \sum l_{i,j} h_{i,j} - \sum v_{i,j} H_{i,j} + \sum f_{i,j} h^F_{i,j} \pm Q_i = \mathcal{D}_p \tag{9}$$

Summation equation

$$\sum \frac{l_{ij}}{L_i} - 1 = \mathcal{D}_p \tag{10}$$

Here $\mathcal{D}_p$ are the discrepancies in the model equations which reduce to zero at the solution.

2. Modeling of Cryogenic Packed Beds

The governing equations for mass and energy balances for the packed cryogenic bed have been reported in literature by Abulhassan et al. [24,25]. Fig. 7 provides a schematic representation of the cryogenic packed bed and the resultant mass and energy balance equations are given below:

The mass balance equation across the bed is given by

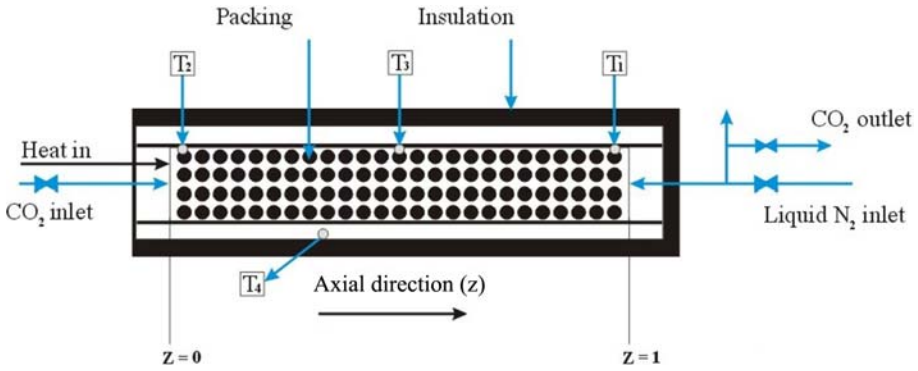

Fig. 7. Schematic diagram for cryogenic packed bed.

$$\varepsilon_g \rho_g \frac{\partial C}{\partial t} = -\rho_g v_g \frac{\partial C_{i,g}}{\partial z} + \frac{\partial}{\partial z}\left(\rho_g D_{eff} \frac{\partial C}{\partial z}\right) - \dot{m}_i'' a_s \tag{11}$$

The energy balance equation across the bed is given by

$$(\varepsilon_g \rho_g C_{pg} + \rho_s(-\varepsilon_g) C_{ps}) \frac{\partial T}{\partial t} = -\rho_g v_g C_{pg} \frac{\partial T}{\partial z} + \frac{\partial T}{\partial z}\left(\lambda_{eff} \frac{\partial T}{\partial z}\right) + \frac{\partial T}{\partial z}\left(k \frac{\partial T}{\partial z}\right) - \sum_{i=1}^{n_c} \dot{m}_i'' a_s h_i \tag{12}$$

Effective axial heat dispersion (λ_{eff}) in a transient packed bed is calculated as

$$\lambda_{eff} = \lambda_g \{1 - (1-\varepsilon_g)^{1/2} + \frac{2(1-\varepsilon_g)^{1/2}}{1-BK}\left[\frac{(1-K)B}{(1-BK)^2} \ln\left(\frac{1}{BK}\right) - \left(\frac{B+1}{2}\right) - \left(\frac{B-1}{1-BK}\right)\right]\} \tag{13}$$

where

$$K = \frac{\lambda_g}{\lambda_s} \tag{14}$$

$$B = 1.364\left(\frac{1-\varepsilon_g}{\varepsilon_g}\right)^{1.055} \tag{15}$$

In the above equations, the porosity of the packed bed is time-dependent. A change in porosity with time is caused due to continuous deposition of CO_2 on the available surface of packing.

The porosity can be defined as:

$$\text{Porosity} = \varepsilon = \frac{\text{Void volume}}{\text{Total volume of bed}} = \frac{V_{void}}{V_T} \tag{16}$$

RESULTS AND DISCUSSION

Four different case studies have been attempted for the separation of CO_2 from natural gas using hybrid cryogenic separation networks. Case study 1 provides simulation of a conventional cryogenic distillation network with feed containing 50 mole% and 72 mole% carbon dioxide. Case studies 2 and 3 provide simulation of a hybrid cryogenic network with feed containing 50 mole% and 72 mole% carbon dioxide, respectively. Only a single cryogenic packed bed is used in these case studies. Case study 4 uses multiple suitably located cryogenic packed beds with feed containing 72 mole% carbon dioxide. The single cryogenic distillation column modeling, which is required in all simulation studies, is validated and reported in the appendix.

Fig. 11 provides the basis for calculation of energy requirement in single cryogenic packed beds as reported in literature by Abulhassan et al. [24]. To investigate the effects of carbon dioxide concentration or loading on the energy requirement, the experimental value was converted into per kg of CO_2 basis. This value is 660 to

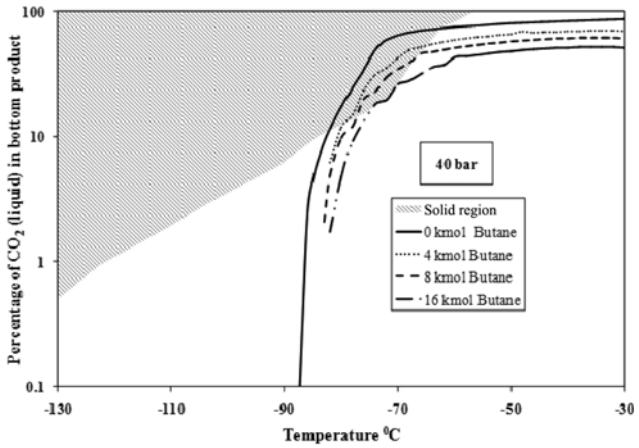

Fig. 8. Separation limit in the presence of additive at 40 bar. The shaded region indicates solid formation [32].

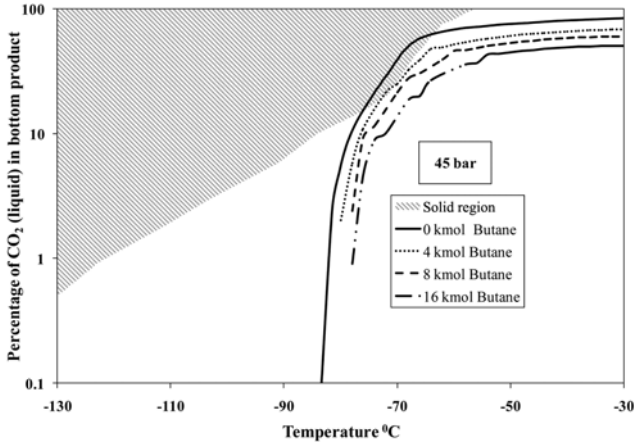

Fig. 9. Separation limit in the presence of additive at 45 bar. The shaded region indicates solid formation [32].

800 kJ/kg of CO_2 based on the experimental controller and switching conditions.

Table 13 provides the energy requirements for conventional, hybrid and multibed hybrid networks. Table 14 provides a comparative cost benefit analysis for hybrid cryogenic distillation networks with 72 mole% of carbon dioxide in the feed. The costs of columns, heat exchangers and packed columns are calculated by the correlations published by Loh and Jennifer Lyons [35] and subsequently updated with Chemical Engineering Plant Cost Index (CEPCI) for 2013. Material of construction has been assumed as stainless steel. The accuracy of capital cost for the network using conceptual cost estimation has an accuracy of 40% as reported in recent literature [36].

1. Case Study 1: Simulation of Conventional Cryogenic Distillation Network in Presence of Additives (Base Case)

Extractive distillation has been successfully employed to overcome the problem of solid formation. This involves adding a heavier hydrocarbon stream to the condenser in a fractionation column. Extractive distillation using heavier hydrocarbons or helium alters the solubility characteristics of the system and produces low percentage of CO_2 in the overhead product.

Simulation analysis was conducted to investigate the theoretical limits of CO_2 separation at different pressures and with different

Table 2. Column data for conventional distillation network with 50 mole% CO_2 in feed

		Column 1	Column2	Column 3	Column 4	Column 5	Column 6
Conventional	Theoretical stages	17	10	40	10	10	40
	Feed stage (from top)	5	5	20	6	5	20
	Additive feed stage no.	n/a	1	1	n/a	n/a	n/a
	Pressure (bar)	40	40	40	40	40	30
	Condenser temperature (°C)	−56.6	−81.2	−87.2	23.6	−11.8	−6.2
	Condenser duty (MW)	64.9	35.2	14.0	18.0	1.3	50.1
	Reflux ratio	1.75	1.6	1.7	1.7	1.6	1.52
	Reboiler temperature (°C)	8.3	22.9	21.7	146.7	79.3	119.1
	Reboiler duty (MW)	22.8	20.3	11.4	32.6	33.7	81.4
	Total duty	386 MW					

Table 3. Column composition for conventional distillation network for feed with 50 mole% CO_2

	Component	Column 1		Column2		Column 3		Column 4		Column 5		Column 6	
		Top	Bottom	Top	Bottom	Top	Bottom	Top	Bottom	Top	Bottom	Top	Bottom
Conventional	CH_4	0.788		0.964	0.005	0.987	0.188	0.007		0.288			
	C_2H_6	0.031	0.039	0.001	0.101		0.027	0.150	0.017	0.035	0.012	0.044	
	C_3H8	0.001	0.048		0.003		0.001	0.003	0.002		0.002	0.007	0.389
	n-C_4H_{10}		0.018	0.001	0.390		0.260	0.068	0.948	0.001	0.750		0.172
	i-C_4H_{10}		0.018										0.172
	n-C_5H_{12}		0.012										0.115
	i-C_5H_{12}		0.012										0.115
	n-C_6H_{14}		0.004										0.038
	CO_2	0.170	0.848	0.022	0.501	338 ppm	0.524	0.771	0.032	0.677	0.236	0.948	
	N_2	0.010		0.012		0.013	0.000						

Table 4. Column data for conventional distillation network with 72 mole% CO_2 in feed

		Column 1	Column 2	Column 3	Column 4	Column 5	Column 6
Conventional	Theoretical stages	17	10	40	10	10	40
	Feed stage (from top)	5	5	20	6	5	20
	Additive feed stage no.	n/a	1	1	n/a	n/a	n/a
	Pressure (bar)	40	40	40	40	40	30
	Condenser temperature (°C)	−31.2	−69.1	−84.7	2.8	−0.5	−5.7
	Condenser duty (MW)	48.3	20.1	11.3	15.0	2.1	67.4
	Reflux ratio	1.75	1.6	1.7	1.7	1.6	1.52
	Reboiler temperature (°C)	7.7	12.4	36.9	139.9	146.8	133.2
	Reboiler duty (MW)	27.4	11.8	10.5	29.0	7.7	109.1
	Total duty	360 MW					

Table 5. Column composition for conventional distillation network for feed with 72 mole% CO_2

		Column 1		Column2		Column 3		Column 4		Column 5		Column 6	
		Top	Bottom	Top	Bottom	Top	Bottom	Top	Bottom	Top	Bottom	Top	Bottom
Conventional	CH_4	0.551		0.893	0.010	0.974	0.038	0.013		0.101	0.001		
	C_2H_6	0.036	0.019	0.005	0.066		0.025	0.084	0.015	0.052	0.009	0.020	
	C_3H8	0.002	0.023		0.012		0.007	0.004	0.035	0.003	0.009	0.005	0.246
	n-C_4H_{10}		0.016	0.001	0.223	0.001	0.585	0.001	0.875	0.005	0.926		0.215
	i-C_4H_{10}		0.016		0.007		0.014		0.026		0.022		0.215
	n-C_5H_{12}		0.008										0.108
	i-C_5H_{12}		0.008				0.001		0.001		0.001		0.108
	n-C_6H_{14}		0.008										0.108
	CO_2	0.398	0.903	0.078	0.682	0.002	0.331	0.899	0.048	0.839	0.032	0.974	
	N_2	0.014		0.023		0.025							

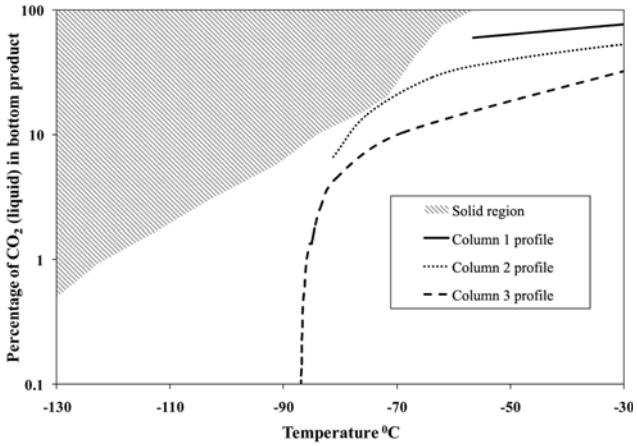

Fig. 10. Profiles of liquid CO_2 in conventional distillation columns network for 50 mole% CO_2. The shaded region indicates solid formation [32].

flow rates of n-Butane. The results of this investigation are presented in Figs. 8 and 9. It is evident that addition of greater amounts of the additives increases the safety margin by moving the theoretical separation line away from the CO_2 solid formation region. The additives also raise the operating temperature of the overhead and increase relative volatility. Also with the increase of column pressure, it is possible to avoid the solidification region without the use of additives. However, the purity of CH_4 decreases as the working pressure is increased.

Table 6. Physical properties of cryogenic packed bed

Diameter of packing	0.01 m
Density of packing	2,000 kg/m^3
Porosity (ε_g)	0.64
Heat capacity of packing	0.84 J/g·K
Heat capacity of shell	0.466 J/g·K

A simulation study was performed using butane as an additive. The feed composition is provided in Table 1 with a flowrate of 24,800 kmol/h [10]. The pressure and temperature before entering the distillation column is considered to be 40 bar and 10 °C, respectively. In the first column the composition of the CO_2 in the top product is reduced to 17% giving 78.8% CH_4 by fixing the distillate flowrate, reflux ratio, total number of plates, feed plate and pressure. The criterion for fixing these variables is to minimize the CH_4 losses.

Column 1 operates without any additives and butane is added as an additive in column 2 and column 3. In the present study, 0.12 kmol additive per kmol of feed (in column 2) and 0.10 kmol additive per kmol of feed (in column 3) have been added. This leads to a purification of methane up to 96.4% in column 2 and 98.7% in column 3, and the loss of methane during this process is approxi-

Table 7. Column data for hybrid distillation network with 50 mole% CO_2 in feed

		Column 5 Packed bed	Column 2	Column 3	Column 4	Column 5
Hybrid	Theoretical stages	n/a	17	40	10	40
	Feed stage (from top)	n/a	5	20	5	20
	Additive feed stage no.	n/a	1	1	n/a	n/a
	Pressure (bar)	40	40	40	40	30
	Condenser temperature (°C)		−69.9	−84.4	−12.8	−7.7
	Condenser duty (MW)		43.3	20.7	4.4	4.7
	Reflux ratio	87.62 MW	1.75	1.6	1.6	1.52
	Reboiler temperature (°C)		69.8	12.2	111.8	108.9
	Reboiler duty (MW)		59.7	16.8	13.4	10.9
	Total duty			262 MW		

mately 1%. The simulated hydrocarbon loss was found to be less than the losses (498.8 kmol/h) reported in literature [10] with n-pentane as additive. Tables 2 and 3 present the distillation column data on the energy requirement and composition. However, these conditions are not optimized with respect to separation, energy requirement, and additive flow rate etc. Fig. 10 shows the liquid CO_2 profile in distillation columns.

The recovery of methane from the third column is 9,752 kmol/h, while the quantity of the methane in the feed was 9.855 kmol/h.

The column data and composition profile and energy data for conventional network with 72 mole% feed are provided in Tables 4 and 5.

It is evident from the solutions of simulation that the pressure, temperature and additive flow profiles in the cryogenic distillation

Table 8. Column composition for hybrid distillation network for feed with 50 mole% CO_2

	Component	Column 1 Packed bed		Column 2		Column 3		Column 4		Column 5	
		Liquid	Solid	Top	Bottom	Top	Bottom	Top	Bottom	Top	Bottom
Hybrid	CH_4	0.709		0.896		0.986	0.104	0.289	0.001		
	C_2H_6	0.067		0.012	0.181		0.048	0.063	0.040	0.385	0.105
	C_3H_8	0.042			0.133					0.019	0.175
	n-C_4H_{10}	0.016		0.001	0.389	0.001	0.536	0.001	0.834		0.535
	i-C_4H_{10}	0.016			0.051						0.069
	n-C_5H_{12}	0.011			0.035						0.048
	i-C_5H_{12}	0.011			0.035						0.048
	n-C_6H_{14}	0.004			0.013						0.017
	CO_2	0.115	1.0	0.079	0.165	60 ppm	0.312	0.647	0.126	0.597	0.003
	N_2	0.009		0.011		0.013					

Table 9. Column data for hybrid distillation network with 72 mole% CO_2 in feed

		Column 1 Packed bed	Column 2	Column 3	Column 4	Column 5
Hybrid	Theoretical stages	n/a	17	20	10	40
	Feed stage (from top)	n/a	5	10	5	20
	Additive feed stage no.	n/a	n/a	1	n/a	n/a
	Pressure (bar)	40	40	40	40	30
	Condenser temperature (°C)		−64.2	−85.0	−1.2	−8.2
	Condenser duty (MW)		25.0	10.3	3.5	9.8
	Reflux ratio	122 MW	1.75	1.6	1.6	1.52
	Reboiler temperature (°C)		20.1	19.1	146.5	115.6
	Reboiler duty (MW)		42.0	7.9	9.4	19.3
	Total duty			249 MW		

Table 10. Column composition for hybrid distillation network for feed with 72 mole% CO_2

		Column 1 Packed bed		Column 2		Column 3		Column 4		Column 5	
		Liquid	Solid	Top	Bottom	Top	Bottom	Top	Bottom	Top	Bottom
Hybrid	CH_4	0.516		0.827		0.974	0.030	0.050			
	C_2H_6	0.069		0.037	0.111	0.001	0.150	0.230	0.035	0.134	0.071
	C_3H_8	0.039			0.104		0.001		0.001	0.008	0.269
	n-C_4H_{10}	0.026			0.070	0.001	0.392	0.003	0.943		0.188
	i-C_4H_{10}	0.026			0.070						0.188
	n-C_5H_{12}	0.013			0.035						0.094
	i-C_5H_{12}	0.013			0.035						0.094
	n-C_6H_{14}	0.013			0.035						0.094
	CO_2	0.272	1.0	0.115	0.541		0.428	0.716	0.020	0.857	0.001
	N_2	0.013		0.021		0.025					

network pose a multi-variable optimization problem which needs to be solved for achieving the optimal combination in the network. A detailed study on optimization of conventional and hybrid networks will be presented in future work.

2. Case Study 2: Simulation of Hybrid Cryogenic Networks Consisting of Single Multibed Separator with Feed Containing 50 mole% Carbon Dioxide

A single cryogenic packed bed was located before the first distillation column. Table 6 provides physical property data for cryogenic packed bed. This resulted in reduction of flowrate of feed to subsequent columns, causing reduction in size and energy requirements. The energy requirement for the cryogenic packed bed was substantially lower compared to conventional distillation columns.

The results for 50 mole% CO_2 feed are presented in Tables 7 and 8. The results show several potential benefits of using hybrid networks in cryogenic separation. Both the energy requirements as well as size requirements for the conventional part of the network decrease significantly by the use of an initial non-conventional separator.

The energy requirement for the hybrid network was found to be 262 MW, while the conventional distillation consumes 386 MW. Hence,

Table 11. Column data for multibed hybrid distillation network with 72 mole% CO_2 in feed

		Column 1 Packed bed	Column 2	Column 3 Packed bed	Column 4	Column 5
Multibed hybrid	Theoretical stages	n/a	17	n/a	20	40
	Feed stage (from top)	n/a	5	n/a	10	20
	Additive feed stage no.	n/a	n/a	n/a	n/a	n/a
	Pressure (bar)	40	40	40	40	30
	Condenser temperature (°C)		−56.0		−88.4	−8.2
	Condenser duty (MW)		25.0		7.4	9.8
	Reflux ratio	122 MW	1.75	5 MW	2.0	1.5
	Reboiler temperature (°C)		44.7		-8.9	115.6
	Reboiler duty (MW)		42.0		5.1	19.3
	Total duty			235 MW		

Table 12. Column composition for multibed hybrid distillation network for feed with 72 mole% CO_2

		Column 1 Packed bed		Column 2		Column 3		Column 4		Column 5	
		Liquid	Solid	Top	Bottom	Top	Bottom	Top	Bottom	Top	Bottom
Multibed hybrid	CH_4	0.5165		0.827		0.925		0.975	0.120		
	C_2H_6	0.0691		0.037	0.111	0.037			0.637	0.134	0.071
	C_3H_8	0.0387			0.104				0.003	0.008	0.269
	n-C_4H_{10}	0.0258			0.070						0.188
	i-C_4H_{10}	0.0258			0.070						0.188
	n-C_5H_{12}	0.0129			0.035						0.094
	i-C_5H_{12}	0.0129			0.035						0.094
	n-C_6H_{14}	0.0129			0.035	0.000					0.094
	CO_2	0.2725	1.0	0.115	0.541	0.015	1.0	0.001	0.240	0.857	0.001
	N_2	0.0129		0.021		0.023			0.025		

Table 13. Energy comparison for conventional, Hybrid and multibed hybrid network

Energy comparison conventional, hybrid and multibed (72% CO_2)						
	Conventional (MW)		Hybrid (MW)		Multibed hybrid (MW)	
	Condenser	Reboiler	Condenser	Reboiler	Condenser	Reboiler
C1	48.2	27.4	Packed	122	Packed	122
C2	20.1	11.8	25.0	42.0	25.0	42.0
C3	11.3	10.5	10.3	7.9	Packed	5.0
C4	15.0	29.0	3.5	9.4	7.4	5.1
C5	2.1	7.7	NA	NA	NA	NA
C6	67.4	109.1	9.8	19.3	9.8	19.3
Total	360		249		235	

			Capital cost																Operating duty		CH_4 Losses	
			Columns								Heat exchanger				Compressor				Energy	Additive	Losses	Loss reduction
			Packed	C 1	C 2	Packed	C 3	C 4	C 5	C 6	Butane recycle to C 2		Butane recycle to C 3		Feed to C 2		Feed to C 3					
											MW	M$	MW	M$	MW	M$	MW	M$	MW	kg/h	kg/h	kg/h
Conventional	Diameter	m	n/a	6.63	4.09	n/a	4.12	6.89	5.49	10.10	5.7	0.22	7.22	0.24	0.12	1.75	0.06	1.23	373	581	3159	0
	Height	m		10.40	6.12		24.48	6.12	6.12	24.48												
	Cost	M $		4.01	1.61		2.95	3.90	2.62	12.23												
Hybrid *	Diameter	m	0.71	6.84	4.05	n/a	n/a	5.89	n/a	5.73	4.5	0.13	n/a		0.07	1.14	n/a		254	464	774	2385
	Height	m		10.40	12.24			6.12		24.48												
	Cost	M $	4.01	3.76	2.49			2.96		5.08												
Multibed *	Diameter	m	0.71	6.84	5.13	0.55	n/a	n/a	n/a	5.73	n/a		n/a		0.07	1.14	0.33	1.32	235.4	n/a	606	2553
	Height			10.40	12.24					24.48												
	Cost	M $	4.01	3.76	2.51	3.40				5.08												

* For packed beds the cost is calculated for eight beds (Four each for capture and recovery cycles)

more than 32% reduction of energy was observed by the use of a hybrid cryogenic network. The hybrid network required fewer columns to produce a similar output composition of 98.6 mole% methane.

3. Case Study 3: Simulation of Hybrid Cryogenic Networks Consisting of Single Multibed Separator Unit with Feed Containing 72 mole% Carbon Dioxide

The hybrid cryogenic network performance consisting of single multibed separator unit with feed containing 72 mole% carbon dioxide was investigated. The results for 72 mole% CO_2 feed are presented in Table 9 and 10.

The increase in carbon dioxide in the feed led to the requirement of less energy consumption as compared to the low carbon dioxide feed. The conventional network showed energy reduction of about 7%, while the hybrid network showed a reduction of 5%.

The energy requirement for the hybrid network was found to be 249 MW, while the conventional distillation consumes 360 MW. Hence, more than 30% reduction of energy was observed by the use of hybrid cryogenic network for the high carbon dioxide feed. The hybrid network required fewer columns to produce similar output composition of 97.4 mole% methane.

4. Case Study 4: Simulation of Hybrid Cryogenic Networks Consisting of Multibed Separators at Two Locations with Feed Containing 72 mole% Carbon Dioxide

The hybrid cryogenic network performance consisting of two suitably located multibed separator units with feed containing 72 mole% carbon dioxide was investigated. The results for hybrid network with two cryogenic packed beds and with 72 mole% CO_2 in feed are presented in Tables 11 and 12.

The energy requirement for this multibed hybrid network was found to be 235 MW, while the conventional distillation consumes 360 MW. Hence, more than 34% reduction of energy was observed by the use of hybrid cryogenic network with two cryogenic packed beds for the high carbon dioxide feed. The hybrid network required fewer columns to produce similar output composition of 97.4 mole% methane.

Table 14 shows substantial benefits for using multiple cryogenic packed beds in hybrid cryogenic networks. The benefits are quantified in terms of reduced equipment size and capital cost, reduced energy requirements, elimination of additive butane requirements and reduction of methane losses. Interestingly, the required flow rate of butane as additive was significantly reduced with the use of hybrid cryogenic networks. For the conventional cryogenic network, 0.12 kmol per kmol of feed is required to avoid solidification in column 2 and 0.14 kmol per kmol of feed is required to avoid solid CO_2 formation in column 3. The additive requirement for the single packed bed hybrid network is required only for column 3 at a rate of 0.10 kmol of additive per kmol of feed. This reduction can be attributed to the reduced flow rate of CO_2 in the columns. For multiple bed hybrid networks, the additive requirement can be avoided completely. The methane loss was also found to be reduced considerably.

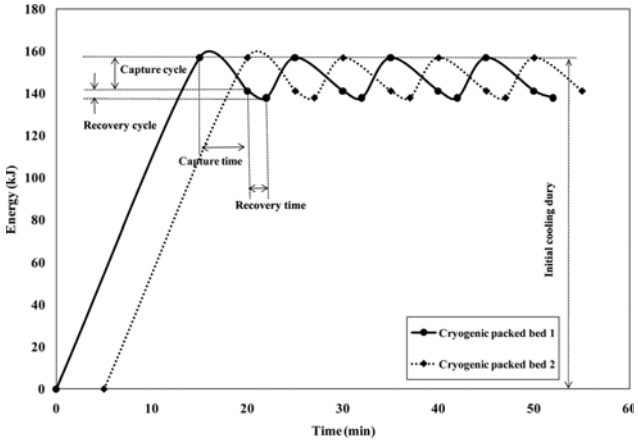

Fig. 11. Energy requirement in a single cryogenic packed bed for desublimation of CO_2 from natural gas (Abulhassan et al., 2014 [24]).

CONCLUSIONS

A hybrid cryogenic network consisting of both conventional and nonconventional technologies has been proposed for minimized energy consumption and size reduction. A base case study comprised of a conventional cryogenic distillation network using butane as an additive was explored for two high carbon dioxide containing natural gas feeds. A conventional cryogenic distillation model has been developed and validated with Aspen Plus. A predictor from experimental data has been embedded in conjunction with the steady state nonlinear (C+3) integral dual loop convergence to avoid formation of CO_2 inside the distillation column. Subsequently, the effects of hybridization were investigated using single and multiple cryogenic packed beds, which were located at suitable positions in the network. It was observed that the optimal number and location of the desublimation based cryogenic packed bed depends on the composition of feed. However, substantial reduction in energy requirement, methane losses and size requirement was observed. It was extremely interesting to note that multiple cryogenic beds eliminate the need for using butane as an extractive distillation additive and reduces the column sizes considerably. The hybrid network showed promising potential for future commercial exploitation through optimization of energy, reduction of hydrocarbon losses and effective size reduction during purification of natural gas.

NOMENCLATURE

$v_{i,j}$: vapor flow rate from the stage
$v_{i+1,j}$: vapor flow rate into the stage from the stage below
S_{ij} : stripping factor
$l_{i,j}$: liquid flow rate from the stage
$l_{i-1,j}$: vapor flow rate into the stage from the stage above
F_i : feed flow at rate i^{th} stage
Q_i : heat flow into or removal from the stage
z : mole fraction of component j in the feed stream
x : mole fraction of component j in the liquid stream
y : mole fraction of component j in the vapor stream
$K_{i,j}$: equilibrium constant for the i^{th} stage, j^{th} component
h, H : enthalpies of liquid and vapor respectively
N : number of stages in the column
C : number of component
t : time [s]
v : superficial velocity [m/s]

z : axial co-ordinate [m]
D_{eff} : effective diffusion coefficient [m^2/s]
$\dot{m}''$: mass deposition rate per unit surface area [$kg/m^2/s$]
a_s : specific solid surface area per unit bed volume [m^2/m^3]
C_p : heat capacity [J/kg/K]
T : temperature [K, °C]
V_T : total volume [m^3]
K : effective axial heat dispersion equation constant $=\lambda_g/\lambda_s$
N_{eqv} : number of packing
V_{eqv} : volume of packing [m^3]
V(t) : time dependent volume of desublimated CO_2 [m^3]
V_F : final volume of desublimated CO_2 [m^3]
m : mass deposition per unit bed volume [kg/m^3]
Re : Reynolds number
Sc : Schmidt number

Greek Letters

ε : bed void fraction
ρ : density [kg/m^3]
ω : mass fraction [kg/kg]
λ_{eff} : effective conductivity [W/m/K]
Δh_i : enthalpy change related to the phase change of component i [J/kg]
τ : residence time [s^{-1}]
$\mathcal{D}_p$: discrepancies

Subscripts

i : index for stage number in distillation model
i : index for component number in packed bed model
j : index for component number
0 : initial
g : gas phase
s : solid phase

REFERENCES

1. J. G. Speight, *Natural Gas A Basic Handbook*, Gulf Publishing Company, Houston, Texas (2007).
2. N. H. Darman and A. R. B. Harum, *Technical challenges and solutions on natural gas development in Malaysia, in: The petroleum policy and management project, 4th Workshop of the China-Sichuan Basin Study*, Beijing, China (2006).
3. D. Dortmundt and K. Doshi, *Recent developments in CO_2 removal membrane technology*, UOP LLC, des Plaines (1999).
4. H. G. Donnelly and D. L. Katz, *Ind. Eng. Chem.*, **46**, 511 (1954).
5. J. Brewer and F. Kurata, *AIChE J.*, **4**, 317 (1958).
6. H. Li, J. P. Jakobsen, Ø. Wilhelmsen and J. Yan, *Appl. Energy*, **88**, 3567 (2011).
7. J. A. Davis, N. Rodewald and F. Kurata, *AIChE J.*, **8**, 537 (1962).
8. A. S. Holmes and J. M. Ryan, *Cryogenic distillative separation of acid gases from methane*, US Patent (1982).
9. A. S. Holmes, J. M. Ryan, B. C. Price and R. E. Styring, *Pilot tests prove out cryogenic acid-gas/hydrocarbon separation processes, in: 61st Annual GPA Convention*, Dallas, TX, March 15-17 (1982).
10. D. Berstad, P. Nekså and R. Anantharaman, *Energy Procedia*, **26**, 41 (2012).
11. J. A. Valencia and R. D. Denton, *Method of separating acid gases, particularly Carbon dioxide from methane by the addition of a light gas such as helium*, US Patent (1983).
12. T. D. Atkinson, J. T. Lavin and D. T. Linnett, *Separation of gaseous in: mixtures*, US Patent (1988).
13. P. S. Northrop and J. A. Valencia, *Energy Procedia*, **1**, 171 (2009).
14. B. T. Kelley, J. A. Valencia, P. S. Northrop and C. J. Mart, *Energy Procedia*, **4**, 824 (2011).
15. A. Hart and N. Gnanendran, *Energy Procedia*, **1**, 697 (2009).
16. M. J. Tuinier, M. van Sint Annaland, G. J. Kramer and J. A. M. Kuipers, *Chem. Eng. Sci.*, **65**, 114 (2010).
17. G. Xu, L. Li, Y. Yang, L. Tian, T. Liu and K. Zhang, *Energy*, **42**, 522 (2012).
18. G. P. Willems, M. Golombok, G. Tesselaar and J. J. H. Brouwers, *AIChE J.*, **56**, 150 (2010).
19. D. Clodic, R. El Hitti, M. Younes, A. Bill and F. Casier, *CO_2 capture by anti-sublimation Thermo-economic process evaluation, in: Fourth Annual Conference on Carbon Capture & Sequestration*, Alexandria, USA, 2 (2005).
20. C.-F. Song, Y. Kitamura, S.-H. Li and K. Ogasawara, *Int. J. Greenhouse Gas Control*, **7**, 107 (2012).
21. C. F. Song, Y. Kitamura and S. H. Li, *Appl. Energy*, **98**, 491 (2012).
22. J. A. Ritter and A. D. Ebner, *Carbon dioxide separation technology: R&D needs for the chemical and petrochemical industries*, Chemical Industry Vision2020 Technology Partnership, in, Oak Ridge National Laboratory (2007).
23. Nor Syahera. M, *Cryogenic separation of CO_2 from methane using dynamic packed bed*, Universiti Teknologi PETRONAS (2012).
24. Abulhassan. A, Nor Syahera M., K. Maqsood and S. Ganguly, *Minimization of energy consumption in counter current switched cryogenic packed beds during purification of natural gas with high carbon dioxide content, Chem. Eng. Technol.* (Revision submitted, 2014).
25. Abulhassan. A, S. Ganguly, and A. B. M. Shariff, *Simulation of cryogenic packed bed using 1-dimensional pseudo homogeneous model, International Oil and Gas Symposium and Exhibition (IOGSE 2013)*, Sabah, Malaysia (2013).
26. K. Maqsood, S. Ganguly and A. B. M. Shariff, *Synthesis of cryogenic distillation networks for maximum methane recovery from natural gas with minimum energy usage*, *International Oil and Gas Symposium and Exhibition (IOGSE 2013)*, Sabah, Malaysia (2013).
27. V. Kumar, A. Sharma, I. R. Chowdhury, S. Ganguly and D. N. Saraf, *Fuel Process. Technol.*, **73**, 1 (2001).
28. R. A. Russel, *Chem. Eng.*, 53 (1983).
29. B. S. Hofeling and J. D. Seader, *AIChE J.*, **24**, 1131 (1978).
30. L. M. Naphtali and D. P. Sandholm, *AIChE J.*, **17**, 148 (1971).
31. T. Eggeman and S. Chafin, *Chem. Eng. Prog.*, 101 (2005).
32. F. Kurata, *Solubility of solid carbon dioxide in pure light hydrocarbons and mixtures of light hydrocarbons*, Research Report RR-10, Gas Processors Association. Tulsa, OK (1974).
33. B. ZareNezhad and T. Eggeman, *Cryogenics*, **46**, 840 (2006).
34. K. Carter and K. D. Luks, *Fluid Phase Equilib.*, **243**, 151 (2006).
35. H. P. Loh, Jenifer Lyons, *Process equipment cost estimation*, DOE, Pittsburgh (2002).
36. M. J. Tuinier, H. P. Hamers and M. van Sint Annaland, *Int. J. Greenhouse Gas Control*, **5**, 1559 (2011).

APPENDIX

1. Simulation of Conventional Cryogenic Distillation in Conjunction with Prediction of Solid Formation

The formulation of MESH equations presented in section 3.1 is referred to as (*C*+3) formulation, since there are (*C*+3) equations in the model and as many variables to be calculated. The matrix form is called block tri-diagonal or quasi tri-diagonal structure. The simple matrix structure enables use of sparse matrix convergence algorithm to reduce memory usage and computation time. The solution is accomplished by a Gaussian elimination scheme and Newton-Raphson convergence with golden section optimization. Fig. 12 shows the schematic flowchart for the solution of the multi-component distillation model.

Thermodynamic correlation and prediction of solid formation are based on interpolation of experimental data available from literature [4-7]. Table 15 provides the details of input specifications and guess values for the simulation experiments.

Fig. 13 shows the liquid and vapor phase of CO_2 composition variations along the column at the convergence for different feed locations. Fig. 14 provides the stagewise temperature variation inside the column and Fig. 15 provides the different convergence characteristics. The use of golden section optimization along with the Newton-Raphson convergence generates very stable convergence profiles.

The results obtained through the proposed MESH model are subsequently compared with the results obtained through simulation using ASPEN PLUS. Table 16 shows a comparison of the values generated using the proposed model along with the simulation data obtained through ASPEN PLUS. An excellent overall match with ASPEN PLUS confirmed that the present formulation is satisfactory.

2. Embedding of Solid Formation Prediction Inside the Convergence Loops

CO_2 and methane have quite high relative volatilities at normal pressure, but at higher pressures CO_2 forms a solid phase inside the distillation column during production of high purity methane. Fig. 16 illustrates the theoretical limits of methane purity which can be obtained in a binary CO_2 and methane system at different pressures without any additives. It is evident from the Fig. 16 that a suitable predictor needs to be implemented in conjunction with the cryogenic distillation model for efficient and meaningful simulation interpretations and results.

Eggeman and Chafin [31] used thermodynamics model sets for the prediction of carbon dioxide freezing points. The Peng-Robinson equation of state was investigated along with the activity coefficient model based on the NRTL. The authors compared the prediction with the experiment data given by Kurata [32]. ZareNezhad and Eggeman [33] predicted carbon dioxide freezing points by using Peng-Robinson equation of state along with the classic mixing rules. The predicted data was compared with the GPSA Data Book and with Kurata [32]. Carter and Luks [34] present a method for

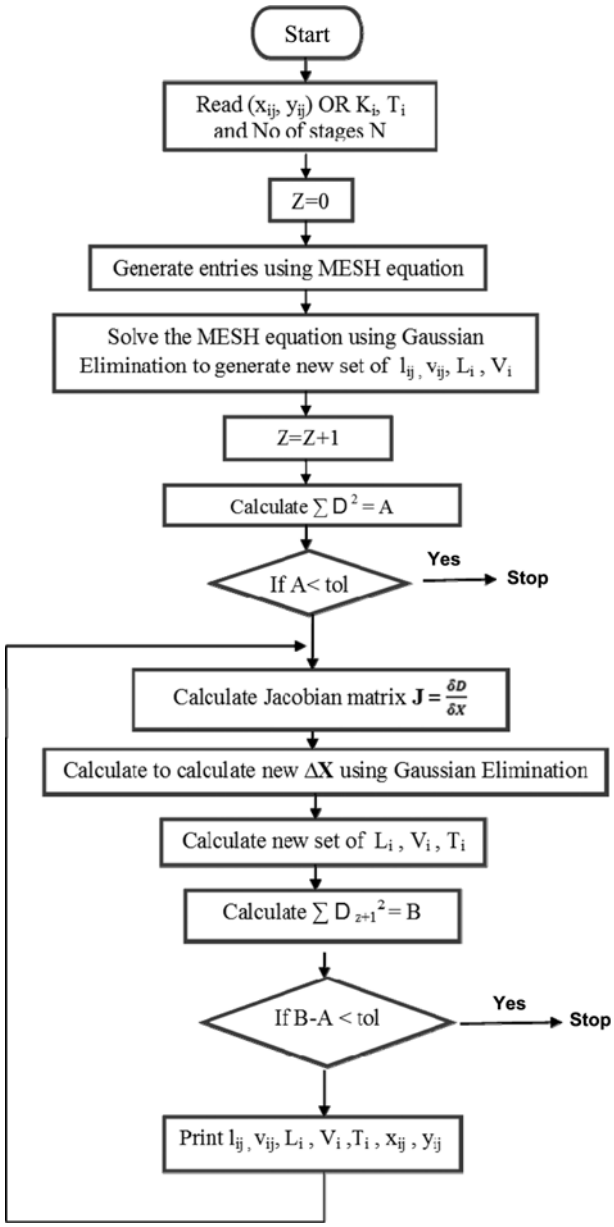

Fig. 12. Flowchart of algorithm for solution of multi-component distillation model.

Table 14. Input specifications for model

Input specifications			
Column pressure	64 atm	No. of theoretical stages (including reboiler and condenser)	10
Feed composition	x_{CO_2}=0.6	Feed stage (from top)	5
	x_{CH_4}=0.4	Reflux	1.2
Feed temperature	−10 °C	Top flowrate	65 mol/h
Feed flowrate	100 mol/h	Bottom flowrate	35 mol/h
Condenser temperature	−50 °C	Reboiler temperature	40 °C (initial guess)

Table 15. Comparison of proposed cryogenic distillation model with ASPEN PLUS

Distillate flow rate	Feed composition CO_2	ASPEN PLUS		Present work	
		Top CO_2	Bottom CO_2	Top CO_2	Bottom CO_2
60	0.7	0.5076	0.9886	0.4967	0.9996
	0.9	No convergence		0.7769	0.9998
55	0.7	0.4672	0.9844	0.4394	0.9993
	0.9	No convergence		0.7514	0.9998
50	0.6	0.3522	0.8478	0.3445	0.9983
45	0.7	0.3826	0.9597	0.3716	0.9983
	0.8	0.5716	0.9869	0.5812	0.9910
40	0.6	0.4278	0.9896	0.4478	0.9913

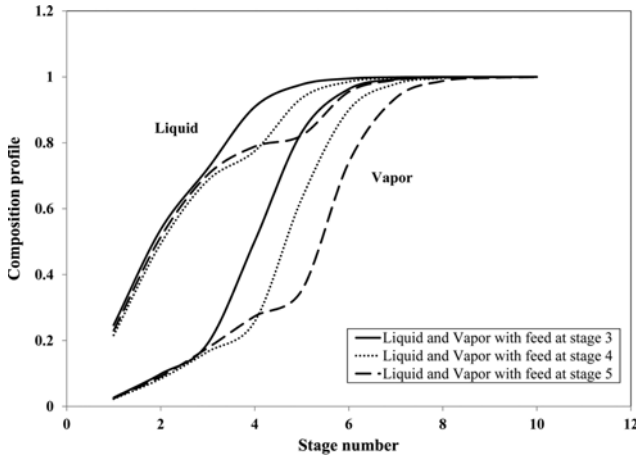

Fig. 13. Mole fraction variation of CO_2 with theoretical plate for different feed location.

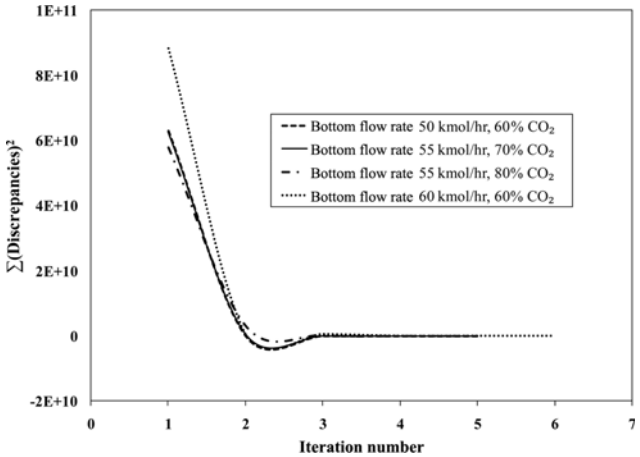

Fig. 15. Variation of Σ(discrepancies)² with iteration number for different CO_2 feed composition.

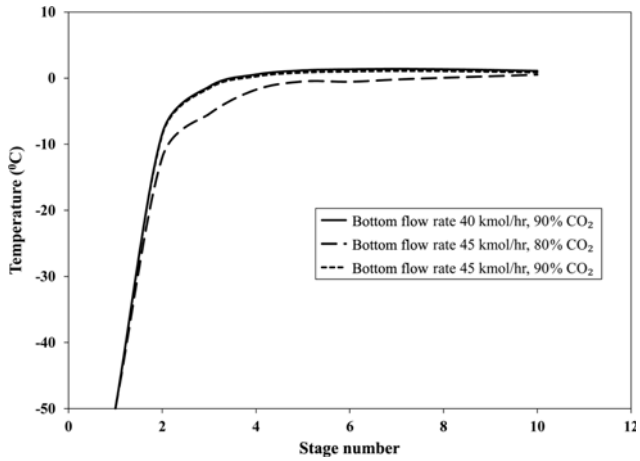

Fig. 14. Temperature variation with theoretical plates with different feed composition.

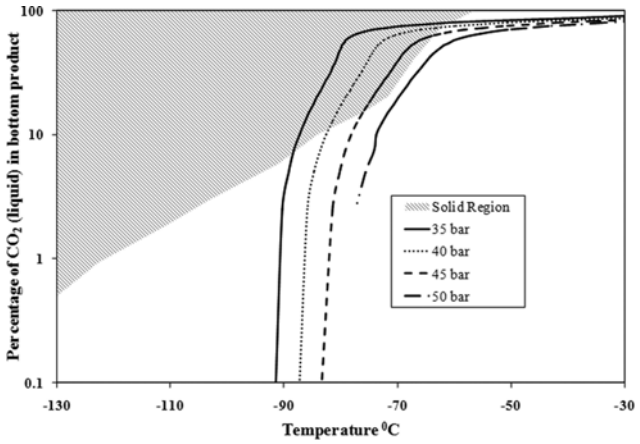

Fig. 16. Theoretical limit of CO_2 separation at different pressure without additives. The shaded region indicates solid formation [32].

describing solid-fluid phase equilibriums of a binary mixture using Soave-Redlich-Kwong equation of state.

In the present work, all the experimental data available in literature was collected into an interpolation table and the prediction of solid formation has been cross-checked at each iteration in convergence and the solid formation zones have been identified and avoided.

It was observed that in the region in which Aspen Plus simulator with PR equation of state failed to converge, the indigenous model with experimental thermodynamic correlation and with solid formation prediction provided smooth convergence. This necessarily shows that in cryogenic regions, the prediction of solid formation and avoiding zones of solid formation during the iterative solution, improves the convergence characteristics of cryogenic distillation simulation.

Table 17. Solid phase prediction at different distillate flow rates in cryogenic distillation column

Distillate flow rate (kmol/h)	Condenser temperature (°C)	Top CO_2 (mole fraction)	Bottom CO_2 (mole fraction)	Predictor output
40	−68.71	0.111	0.926	Solid phase exist
45	−67.37	0.117	0.995	Solid phase exist
50	−52.46	0.200	0.9996	Solid Phase avoided

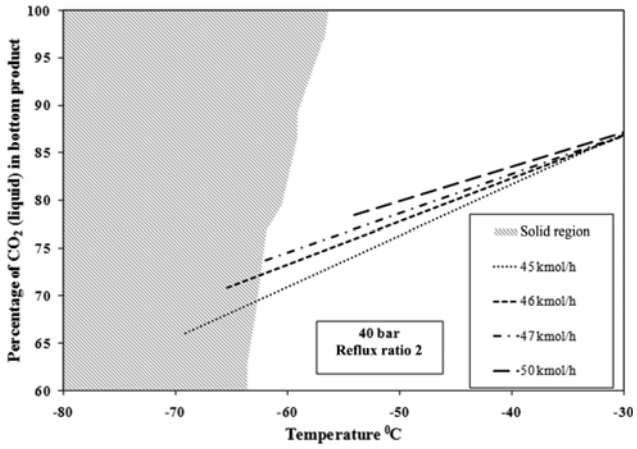

Fig. 17. Solid CO_2 avoidance by changing distillate flow rate. The shaded region indicates solid formation [32].

A representative simple example of avoiding solid formation inside the cryogenic distillation column during mathematical convergence is given in Table 17. It is evident that increase of distillate flow rate and reduction of condenser temperature avoided formation of solids CO_2 and a convergence result was smoothly obtained. Fig. 17 explains how solidification of CO_2 in the cryogenic distillation column can be avoided by increasing the distillate flow rate. It is evident from this section that a predictor for avoidance of solid CO_2 needs to be embedded in the optimizer in conjunction with the cryogenic distillation model or during execute of optimizer.